J|A|C|S
ARTICLES
Published on Web 10/07/2006

Solvent Effects in Thermodynamically Controlled Multicomponent Nanocage Syntheses

Xuejun Liu and Ralf Warmuth*

Contribution from the Department of Chemistry and Chemical Biology, Rutgers, The State University of New Jersey, Piscataway, New Jersey 08854

Received June 23, 2006; E-mail: warmuth@rutgers.edu.

Abstract: The solvent effects on the condensation reaction between tetraformylcavitand **2** and ethylene-1,2-diamine **3** are reported. Earlier, it was found that the trifluoroacetic acid-catalyzed condensation of **2** and 2 equiv of **3** in $CHCl_3$ provides in 82% yield an octahedral nanocage **1** composed of 6 cavitands that are linked together by 12 $-CH{=}N-CH_2CH_2-N{=}CH-$ linker groups (Liu, X.; Liu, Y.; Li, G.; Warmuth, R. *Angew. Chem., Int. Ed.* **2006**, *45*, 901). In tetrahydrofuran, the same reactants yield a tetrameric nanocage **4** (35% yield), which resembles a distorted tetrahedron built up from four cavitands that occupy the apexes. Each cavitand is doubly linked to one other cavitand and singly linked to the other two cavitands via $-CH{=}N-CH_2CH_2N{=}CH-$ connectors. In CH_2Cl_2, the reaction between 8 **2** and 16 **3** yields a square antiprismatic nanocage **5** (65% yield), in which each cavitand occupies one of the eight corners and is connected to four neighboring cavitands via $-CH{=}N-CH_2CH_2-N{=}CH-$ linkers. Nanocage **5** is also the main product in CH_2ClCH_2Cl (26% yield) and $CHCl_2CHCl_2$ (33% yield). Reduction of all imine bonds in **4** and **5** yields polyaminonanocontainers **7** and **8**, respectively, which were isolated as trifluoroacetate salts. Contrary to the formation of larger capsules composed of four, six, or eight cavitands in the reaction between **2** and **3**, the acid-catalyzed reaction of **2** with 2 equiv of $H_2N-X-NH_2$ (X = $(CH_2)_{n=3,4,5}$, 1,3-C_6H_4, 1,4-$(CH_2)_2C_6H_4$, or 1,3-$(CH_2)_2C_6H_4$) quantitatively yields octaiminohemicarcerands **9**−**14**, in which two cavitands are connected with four $-CH{=}N-X-N{=}CH-$ linkers. The outcomes of these condensation reactions are rationalized with the different diamine structures and the relative orientation of cavitands in **1**, **4**, **5**, and **9**−**14**.

Introduction

The efficient synthesis of molecular containers that are large enough to encapsulate multiple guests is a great challenge.[1−5] Molecular containers[6] are of great interest as nanoreactors,[7] in which fleeting intermediates are stabilized,[8] reactions are accelerated,[9] and regio- and stereochemistry are altered,[10] to probe weak interactions,[11] for solar energy conversion,[12] nanodevice fabrication,[13] delivery,[14] storage, and separation technology.[15]

In a recent communication, we reported the one-pot synthesis of an octahedral nanocage **1** from 6 tetraformylcavitands **2** and 12 ethylene-1,2-diamines (**3**) in high yield by making use of dynamic covalent chemistry (Chart 1).[1] This approach strongly

(1) Liu, X.; Liu, Y.; Li, G.; Warmuth, R. *Angew. Chem., Int. Ed.* **2006**, *45*, 901−904.
(2) (a) Barrett, E. S.; Irwin, J. L.; Edwards, A. J.; Sherburn, M. S. *J. Am. Chem. Soc.* **2004**, *126*, 16747−16749. (b) Makeiff, D. A.; Sherman, J. C. *J. Am. Chem. Soc.* **2005**, *127*, 12363−12367.
(3) (a) Sherman, J. *Chem. Commun.* **2003**, 1617−1623. (b) Rissanen, K. *Angew. Chem., Int. Ed.* **2005**, *44*, 3652−3654.
(4) (a) Hof, F.; Craig, S. L.; Nuckolls, C.; Rebek, J., Jr. *Angew. Chem., Int. Ed.* **2002**, *41*, 1488−1508. (b) Mateos-Timoneda, M. A.; Crego-Calama, M.; Reinhoudt, D. N. *Chem. Soc. Rev.* **2004**, *33*, 363−372. (c) MacGillivray, L. R.; Atwood, J. L. *Angew. Chem., Int. Ed.* **1999**, *38*, 1018−1033. (d) MacGillivray, L. R.; Atwood, J. L. *Nature* **1997**, *389*, 469−472. (e) Shivanyuk, A.; Rebek, J., Jr. *Chem. Commun.* **2001**, 2424−2425. (f) Prins, L. J.; Huskens, J.; De Jong, F.; Timmerman, P.; Reinhoudt, D. N. *Nature* **1999**, *398*, 498−502. (g) Prins, L. J. De Jong, F. Timmerman, P. Reinhoudt, D. N. *Nature* **2000**, *408*, 181−184. (h) Ugono, O.; Holman, K. T. *Chem. Commun*. **2006**, 2144−2146.
(5) (a) Fujita, M.; Tominaga, M.; Hori, A.; Therrien, B. *Acc. Chem. Res*. **2005**, *38*, 371−380. (b) Seidel, S. R.; Stang, P. J. *Acc. Chem. Res.* **2002**, *35*, 972−983. (c) Takeda, N.; Umemoto, K.; Yamaguchi, K.; Fujita, M. *Nature* **1999**, *398*, 794−796. (d) Olenyuk, B.; Whiteford, J. A.; Fechtenkoetter, A.; Stang, P. J. *Nature* **1999**, *398*, 796−799. (e) Olenyuk, B.; Levin, M. D.; Whiteford, J. A.; Shield, J. E.; Stang, P. J. *J. Am. Chem. Soc.* **1999**, *121*, 10434−10435. (f) Tominaga, M.; Suzuki, K.; Murase, T.; Fujita, M. *J. Am. Chem. Soc.* **2005**, *127*, 11950−11951.
(6) (a) Cram, D. J.; Cram, J M. *Container Molecules and their Guests*; Royal Society of Chemistry: Cambridge, UK, 1994. (b) Jasat, A.; Sherman, J. C. *Chem. Rev.* **1999**, *99*, 931−967. (c) Warmuth, R.; Yoon, J. *Acc. Chem. Res.* **2001**, *34*, 95−105.
(7) Warmuth, R. *J. Incl. Phenom.* **2000**, *37*, 1−38. Lützen, A. *Angew. Chem., Int. Ed.* **2005**, *44*, 1000−1002.
(8) (a) Cram, D. J.;Tanner, M. E.; Thomas, R. *Angew. Chem., Int. Ed. Engl.* **1991**, *30*, 1024−1027. (b) Warmuth, R. *Angew. Chem., Int. Ed. Engl.* **1997**, *36*, 1347−1350. (c) Warmuth, R. *J. Am. Chem. Soc.* **2001**, *123*, 6955−6956. (d) Liu, X.; Chu, G.; Moss, R. A.; Sauers, R. R.; Warmuth, R. *Angew. Chem., Int. Ed.* **2005**, *44*, 1994−1997. (e) Ziegler, M.; Brumaghim, J. L.; Raymond, K. N. *Angew. Chem., Int. Ed.* **2000**, *39*, 4119−4121.
(9) (a) Kang, J.; Rebek, J., Jr. *Nature* **1996**, *385*, 50−52. (b) Fiedler, D.; Bergman, R. G.; Raymond, K. N. *Angew. Chem., Int. Ed.* **2004**, *43*, 6748−6751. (c) Warmuth, R.; Kerdelhué, J.-L.; Sánchez Carrera, S.; Langenwalter, K. J.; Brown, N. *Angew. Chem., Int. Ed.* **2002**, *41*, 96−99.
(10) (a) Yoshizawa, M.; Takeyama, Y.; Kusukawa, T.; Fujita, M. *Angew. Chem., Int. Ed.* **2002**, *41*, 1347−1349. (b) Warmuth, R.; Maverick, E. F.; Knobler, C. B.; Cram, D. J. *J. Org. Chem.* **2003**, *68*, 2077−2088.
(11) (a) Yoshizawa, M.; Kumazawa, K.; Fujita, M. *J. Am. Chem. Soc.* **2005**, *127*, 13456−13457. (b) Rechavi, D.; Scarso, A.; Rebek, J., Jr. *J. Am. Chem. Soc.* **2004**, *126*, 7738−7739. (c) Rebek, J. Jr. *Angew. Chem., Int. Ed.* **2005**, *44*, 2068−2078.
(12) Pagba, C.; Zordan, G.; Galoppini, E.; Piatnitski, E. L.; Hore, S.; Deshayes, K.; Piotrowiak, P. *J. Am. Chem. Soc*. **2004**, *126*, 9888−9889.
(13) Menozzi, E.; Pinalli, R.; Speets, E. A.; Ravoo, B. J.; Dalcanale, E.; Reinhoudt, D. N. *Chem.−Eur. J.* **2004**, *10*, 2199−2206.
(14) Gibb, C. L. D.; Gibb, B. C. *J. Am. Chem. Soc.* **2004**, *126*, 11408−11409.
(15) Mough, S. T.; Goeltz, J. C.; Holman, K. T. *Angew. Chem., Int. Ed.* **2004**, *43*, 5631−5635.

10.1021/ja0644733 CCC: $33.50 **© 2006 American Chemical Society**

Chart 1

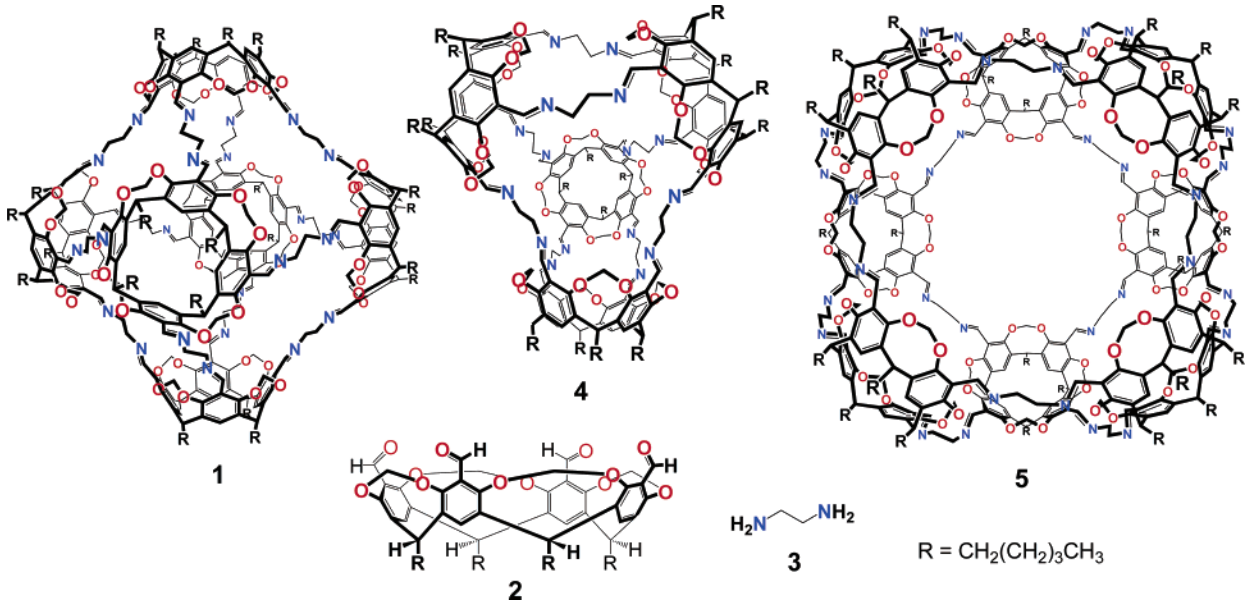

surpasses earlier multistep covalent synthesis in its simplicity and efficiency.[2] Dynamic covalent chemistry offers great advantages in multicomponent syntheses of complex molecules.[16−19] The reversibility of imine bond forming steps that connect reaction components provides an error correction mechanism guaranteeing the ultimate formation of the thermodynamically most stable product **1**. The extension of the dynamic covalent chemistry approach for the synthesis of covalent nanocages leading to novel capsule geometries, and their subsequent functionalization for specific applications needs to be demonstrated.

Here, we report results of a more detailed investigation of the condensation reaction between cavitand **2** and ethylene-1,2-diamine **3**. We specifically aimed at answering the following questions related the multicomponent synthesis of nanocage **1**. (a) What is the effect of the bulk solvent on the stability of octahedral nanocage **1**? (b) Is it possible to direct the assembly to smaller or larger container molecules through a proper solvent choice? (c) What is the mechanism of nanocage formation? Our investigation of the solvent effect led to the discovery of two new nanocages **4** and **5**. Nanocage **4** can be described as a distorted tetrahedron and is built-up from four cavitands and eight linkers, which are connected through 16 newly formed imine bonds. It is the covalent analogue of a coordination tetrahedron that has been reported recently by Beer and coworkers and that is built up from four cavitands linked together by eight Cu(II) ions.[20] The second nanocage **5** is the condensation product of 8 cavitands and 16 diamines held together by 32 imine bonds. It resembles a square antiprism, whose corners are occupied by cavitands. To our knowledge, this square antiprismatic cage is the largest molecule that has been synthesized in a one-pot reaction involving dynamic covalent chemistry.

Results and Discussion

Condensation in Tetrahydrofuran (THF). Contrary to our earlier observations in chloroform (vide infra),[1] the reaction of **2** with **3** in THF containing catalytic amounts of TFA (2.5 mol % per amine) gave only small amounts of octahedral **1** (5% yield) as judged from the ^{1}H NMR spectrum of the crude products after 2 days (Figure 1a).[21] Gel permeation chromatography (GPC) showed a molecular weight shift toward condensation products composed of four cavitands and eight linkers (Calc. MW 3909; Figure 2a). The MALDI-TOF mass spectrum of the crude products after reduction of all imine bonds with $NaBH_4$ further supported this conclusion and showed strong signals for the protonated reduced tetrameric condensation product and its Na^+ adduct (see Supporting Information).

Isolation of this main product (31% yield) was possible by reversed-phase HPLC. The isolated product gave rise to a clean MALDI-TOF mass spectrum. The mass of the two observed isotopic ion clusters are consistent with the proton and sodium adduct of the reduced tetrameric condensation product (Figure 3). We assign this major product to the tetrahedral nanocage **7** (Scheme 1).[22] Views along the two C_2 axes of energy minimized structures of protonated **7**·16H$^+$ are shown in Figure 4 (Amber*,[23] GB/SA water-solvation model[24]). Nanocage **7** has

(16) (a) Rowan, S. J.; Cantrill, S. J.; Cousins, G. R. L.; Sanders, J. K. M.; Stoddart, J. F. *Angew. Chem., Int. Ed.* **2002**, *41*, 898−952. (b) Lehn, J.-M. *Chem. Eur. J.* **1999**, *5*, 2455−2463.
(17) (a) Ro, S.; Rowan, S. J.; Pease, A. R.; Cram, D. J.; Stoddart, J. F. *Org. Lett.* **2000**, *2*, 2411−2414. (b) Quan, M. L. C.; Cram, D. J. *J. Am. Chem. Soc.* **1991**, *113*, 2754−2755.
(18) (a) Chichak, K. S.; Cantrill, S. J.; Pease, A. R.; Chiu, S.-H.; Cave, G. W. V.; Atwood, J. L.; Stoddart, J. F. *Science* **2004**, *304*, 1308−1312. (b) Wang, L.; Vysotsky, M. O.; Bogdan, A.; Bolte, M.; Bohmer V. *Science* **2004**, *304*, 1312−1314. (c) Leung, K. C.-F.; Arico, F.; Cantrill, S. J.; Stoddart, J. F. *J. Am. Chem. Soc.* **2005**, *127*, 5808−5810. (d) Kilbinger, A. F. M.; Cantrill, S. J.; Waltman, A. W.; Day, M. W.; Grubbs, R. H. *Angew. Chem., Int. Ed.* **2003**, *42*, 3281−3285.
(19) (a) R. T. S Lam, A. Belenguer, S. L. Roberts, C. Naumann, T. Jarrosson, S. Otto, J. K. M. Sanders, *Science* **2005**, *308*, 667−669. (b) West, K. R.; Bake, K. D.; Otto, S. *Org. Lett.* **2005**, *7*, 2615−2618.
(20) Fox, O. D.; Drew, M. G. B.; Beer, P. D. *Angew. Chem., Int. Ed.* **2000**, *39*, 135−140.
(21) Control experiments showed that the amount of **1** did not increase during the NMR experiment in $CDCl_3$.
(22) The intercalated dimeric hemicarcerand $\mathbf{15}_2$, whose structure would also be consistent with the observed NMR spectra, was excluded as a possible main product based on the absence of octaimino hemicarcerand **15** (**VI** with X = CH_2CH_2, Scheme 2) formation in these condensation reactions and modeling studies that suggest large steric interactions in $\mathbf{15}_2$.
(23) McDonald, D. Q.; Still, W. C. *Tetrahedron Lett.* **1992**, *33*, 7743−7745.
(24) Still, W. C.; Tempczyk, A.; Hawley, R. C.; Hendrickson, T. *J. Am. Chem. Soc.* **1990**, *112*, 6127−6129.

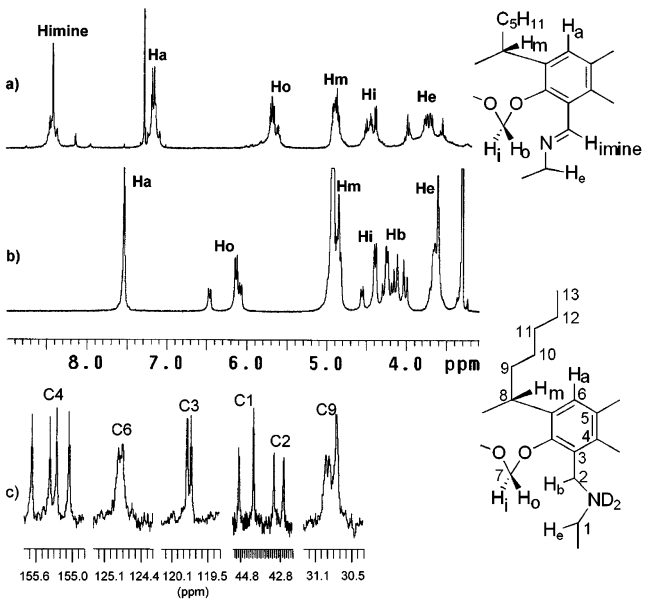

Figure 1. Partial ^{1}H NMR spectra (400 MHz; 22 °C) of (a) crude products formed in the reaction of **2** with 2 equiv of **3** in the presence of 10 mol % TFA in THF after 2 days (in $CDCl_3$; signals assigned to **4** are marked) and (b) of **7**·16CF_3COOH in CD_3OD. (c) Partial ^{13}C NMR spectra (100 MHz, 22 °C, CD_3OD) of **7**·16CF_3COOH.

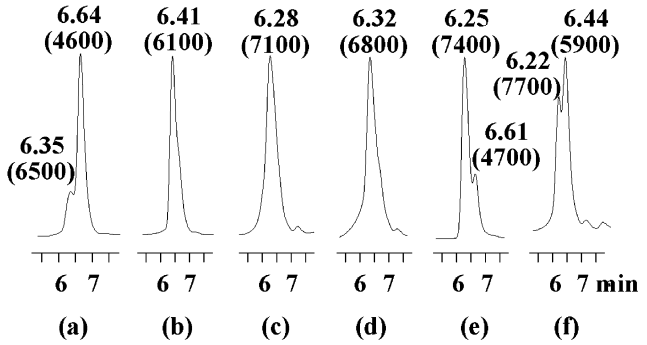

Figure 2. Gel permeation chromatograms of the crude products formed after 2 days in the TFA-catalyzed reaction of **2** with 2 equiv of **3** in (a) THF, (b) $CHCl_3$, (c) CH_2Cl_2, (d) CH_2ClCH_2Cl, and (e) CCl_2HCCl_2H. (f) Products formed in CH_2Cl_2 spiked with **6**. Retention time (in minutes) and estimated molecular weight (in parentheses) are reported for main peaks.

a distorted tetrahedral structure, in which each cavitand is doubly linked to another cavitand at the 1 and 2 position and singly linked to the remaining two cavitands resulting in four larger, nearly spherical portals of approximately 7−8 Å diameter and two smaller elliptically shaped portals. The inner cavity measures approximately 450 Å^3 and was estimated from the volume of the tetrahedron that is formed by connecting the centers of each cavitand.

The structural assignment rests on the ^{1}H and ^{13}C NMR spectra of **7**, which are consistent with its D_{2d} symmetry. Ideally, the ^{1}H NMR spectrum of **7** should show three different outward and inward pointing acetal protons (H_o, H_i) and three different methine protons (H_m) each in a ratio 4:8:4. Furthermore, two singlets for the aryl protons (H_a) (ratio 8:8) and two sets of AB spin systems for the benzylic linker protons (H_b) and another set for the ethylene protons (H_e) are expected (each ratio 16:16). Strong signal overlap in the ^{1}H NMR spectrum of **7**·16CF_3-COOH prevented direct identification of most of these multiplets. Nevertheless, clearly separated are the three doublets at

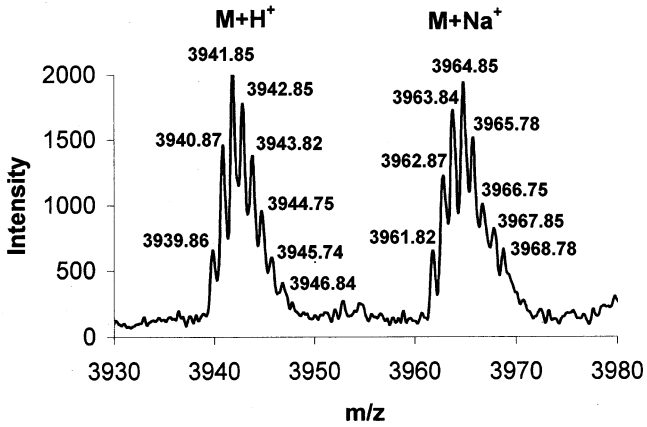

Figure 3. MALDI-TOF mass spectrum of **7**.

6.45, 6.14, and 6.08 ppm (integration ratio 1:2:1) assigned to H_o, which couple to three doublets at 4.58, 4.40, 4.39 ppm (integration ratio 1:2:1) assigned H_i (see Figure 3b and Supporting Information). Well separated are also the two AB systems at 4.26 and 4.21 ppm and 4.13 and 4.02 ppm (integration ratio 1:1) assigned to the benzylic linker protons of **7**. In the ^{13}C NMR spectrum of **7**·16CF_3COOH, the expected number of ^{13}C signals are observed for C1−C4, C6, C7, and C9 (Figure 3c and Supporting Information). For example, four signals (ratio 1:1:1:1) are expected and observed for C4, three signals in a ratio 1:1:2 for C7 and C9, and two signals with equal intensity for C1−C3 and C6. Insufficient signal dispersion led to signal overlap for the remaining carbons C5, C8, and C10−C13.

A full assignment of all proton signals of hexadecaimino cage **4** (Chart 1) in the ^{1}H NMR spectrum of the crude reaction mixture was not possible (Figure 1a). Based on the approximate yield of **4** and consistent with NMR spectra of condensation reactions in different solvents leading to lower yields of **4** (vide infra), we assign the broad singlet at 8.41 ppm to the 16 imine protons, the singlets at 7.18 and 7.15 ppm to 16 H_a and the doublets at 4.49, 4.42, and 4.37 ppm to 16 H_i of **4**.

Condensation in Dichloromethane. Even though chloroform and dichloromethane have very similar solvent properties, the outcome of the condensation reaction in both solvents differed considerably. In dichloromethane, the reaction of **2** with two equivalents of **3** gave the octameric nanocage **5** in 65% yield as the major condensation product and only small amounts of hexamer **1** (5%) (Figure 5a).[21]

GPC of the reaction mixture clearly showed that the main condensation product has a molecular weight of approximately 8000, distinctively higher than that of **1** (Figure 2b,c,f). The formation of a nanocontainer that is built-up from 8 cavitands and 16 ethylene-1,2-diamines connected via 32 newly formed imine bonds is supported by the spectroscopic properties of **5** as well as those of its reduction product **8** (Scheme 1). After reduction of all imine bonds with $NaBH_4$, the main product **8** was isolated in 25% yield as TFA salt by reversed phase HPLC. The MALDI-TOF mass spectrum of **8** shows the expected mass and isotopic pattern for the protonated molecular ion (Figure 6).

We propose the structure shown in Scheme 1 and Chart 1 for **8**. It can be described as a molecular square antiprism, in which the cavitand building blocks occupy the corners and are connected together by sixteen linkers along the prism edges.

Scheme 1. 12-, 18-, and 24-Component Syntheses of Tetrahedral, Octahedral, and Square Antiprismatic Nanocages **4**, **1**, and **5** and Their Reduction

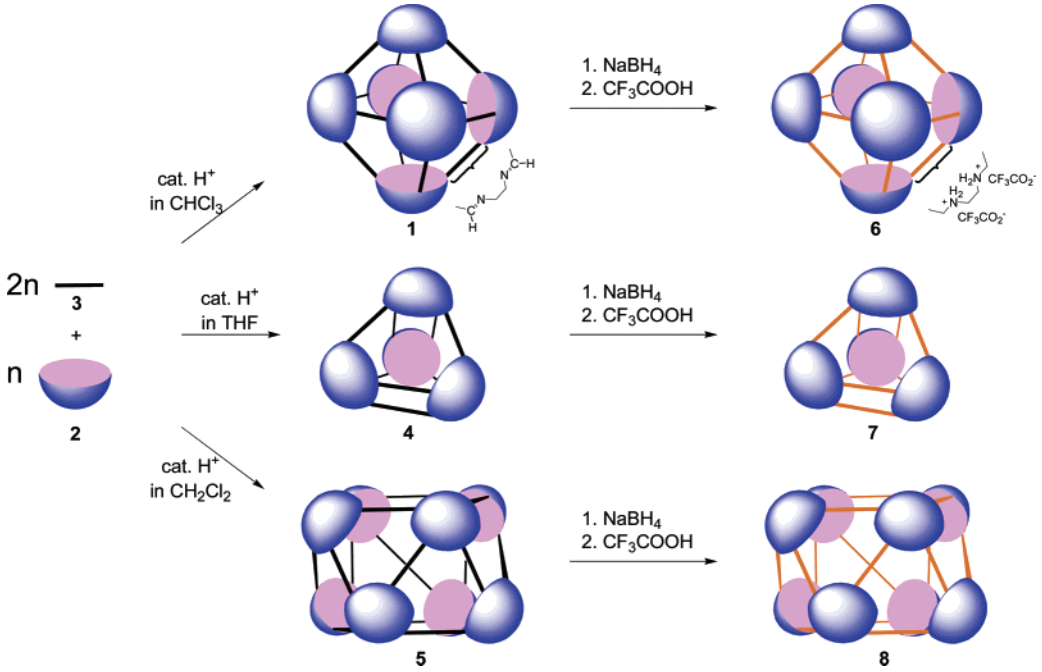

The ^{1}H and ^{13}C NMR spectra of **8**·32CF_3COOH are fully consistent with this structure. Octamer **8** has D_{4d} symmetry, which leads to a similar splitting of the different types of protons and carbons as described for **7**. In other words, **8** has two types of aryl-CH_2NH-CH_2 units (ratio 1:1) and three types of feet and acetal groups (ratio 1:1:2). Due to line broadening and low signal dispersion, signals strongly overlapped in the ^{1}H and ^{13}C NMR spectra of **8**·32CF_3COOH. However, the observation of four different C4 signals (ratio 1:1:1:1), three different C10 signals (ratio 1:1:2), a set of two lines (ratio 1:1) for each C1, C2, and C3 in the ^{13}C NMR spectrum (Figure 5c), and two multiplets (ratio 32:32) for the ethylene protons H_e at 3.57, and 3.61 ppm in the ^{1}H NMR spectrum (Figure 5b), clearly supports the square antiprism structure of **8**.

Greater ^{1}H signal dispersion is observed for the polyimino square antiprism **5**. Based on the analysis of ^{1}H NMR spectra that were recorded before the condensation reaction reached equilibrium and that contained lower amounts of **5**, we assign the two singlets at 8.45 and 8.13 ppm (ratio 16:16) to the 32 imine protons of **5**, the singlet at 7.08 ppm to 16 aryl protons H_a,[25] the doublets at 5.82 and 5.58 ppm (ratio 8:24) to the 32

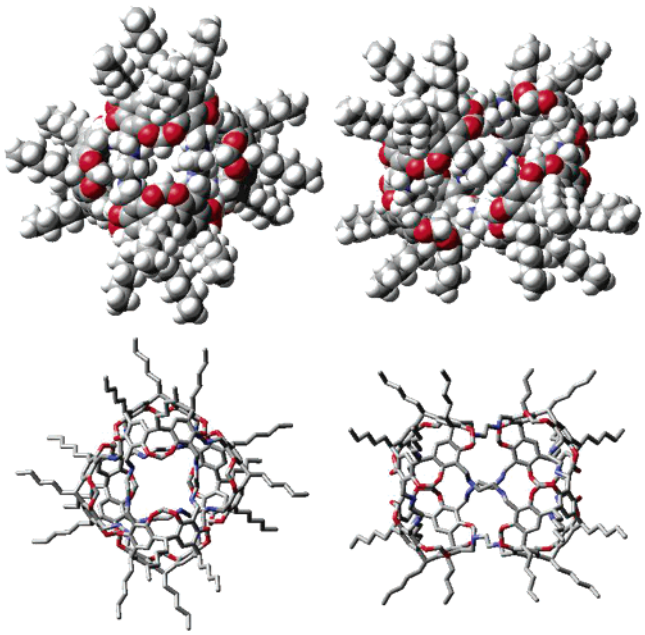

Figure 4. Views along the two C_2 axes of energy-minimized structure of **7**·16H^+ (Amber*,[23] GB/SA water-solvation model[24]). Atom coloring: C, gray; H, white; O, red; N, blue.

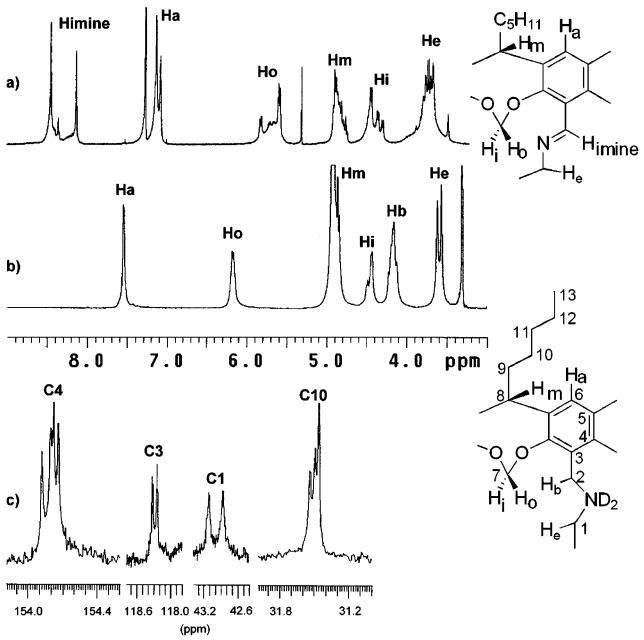

Figure 5. Partial ^{1}H NMR spectra (400 MHz; 22 °C) of (a) crude products formed in the reaction of **2** with 2 equiv of **3** in the presence of 10 mol % TFA in CH_2Cl_2 after 67 h (in $CDCl_3$; signals assigned to **5** are marked) and (b) of **8**·32CF_3COOH in CD_3OD. (c) Partial ^{13}C NMR spectra (100 MHz, 22 °C, CD_3OD) of **8**·32CF_3COOH.

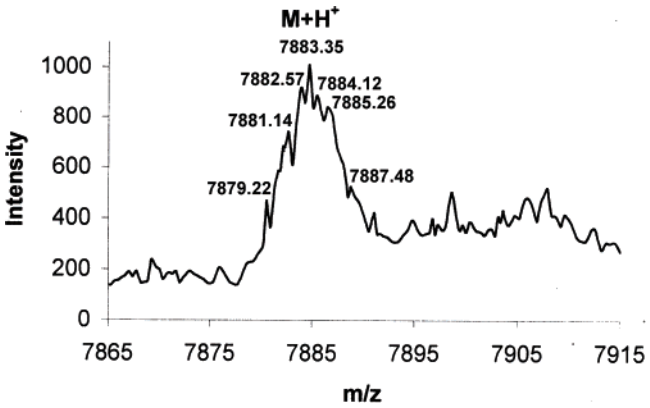

Figure 6. MALDI-TOF mass spectrum of **8**.

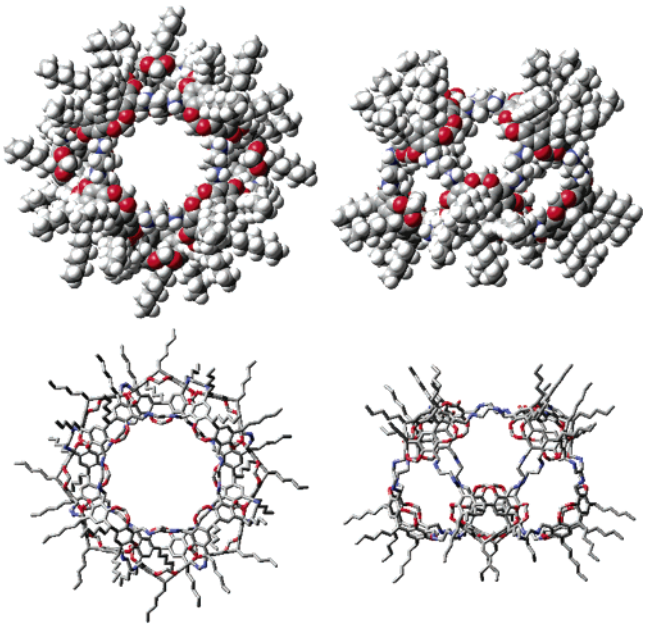

Figure 7. Top and side view of energy-minimized space-filling structure of **8**−32H$^+$ (Amber*,[23] GB/SA water-solvation model[24]). Atom coloring: C, gray; H, white; O, red; N, blue.

outer acetal protons H_o, the doublets at 4.44, 4.36 and 4.30 ppm (ratio 16:8:8) to the 32 inner acetal protons H_i (Figure 5a).

An energy-minimized structure of **8**·32H$^+$ using molecular mechanics calculation is shown in Figure 7. The shape of **8** resembles that of a donut or short nanotube with two larger nearly spherical openings that have diameters of approximately 12 Å. The volume of the disk shaped cavity is approximately 3600 Å^3 and was estimated by comparing it to that of a square antiprism whose corners are located in the centers of the host's cavitands.

Condensation in Chloroform. Even though chloroform and dichloromethane have very similar solvent properties, the outcome of the condensation reaction in both solvents differed considerably. As reported in our earlier communication,[1] the acid-catalyzed reaction of **2** with 2 equiv of **3** in $CHCl_3$ yielded octahedral **1** in 82% yield. The ^{1}H NMR spectrum of the final reaction mixture also showed the presence of approximately 5% tetramer **4**. The reaction reached the final equilibrium after approximately 2 days. Extended reaction times (greater 4 days)

(25) The singlet assigned to the remaining 16 aryl protons is part of the broad singlet at 7.13 ppm.

Scheme 2. Proposed Intramolecular Catalysis of Acetal Spanner Cleavage

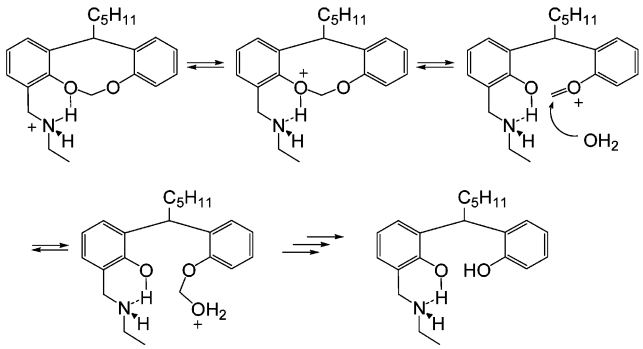

lead to a slow decrease in the yield of **1** and **4**. The rate of this decomposition was acid dependent and might involve acid-catalyzed cleavage of the acetal groups of **1** and **4**. Reduction of the imine bonds of **1**, as described for **4** and **5**, gave **6**, which was isolated in 65% yield by HPLC.

The substantially lower yield of isolated **6** (65%) and **8** (25%) as compared to the yields of **1** (82%) and **5** (65%), respectively, is a consequence of partial decomposition of **6** and **8** during the acidic workup of the reduction step and of the difficulty to separate off these byproducts. ^{1}H NMR and mass spectra show that the reduction of all imine bonds of **1**, **4**, and **5** is quantitative and leads initially to boramines HN−BH_2. Acid-catalyzed hydrolysis of the latter is slow and is accompanied by substantial cleavage of the OCH_2O acetal spanners of the cavitands, if the polyboramino cages are heated in methanol/concentrated HCl (9:1). At room temperature, acetal cleavage is reduced, but still leads to approximately 1−2% cleavage of all acetal groups. Thus, after essentially complete hydrolysis of all HN−BH_2 groups, about 20 and 50% of **6** or **8** in the crude hydrolysis mixtures lack one or more acetals. During the reversed phase HPLC chromatographic purification, these byproducts eluted slightly later than **6** and **8**. In contrast to **6** and **8**, the extent of acetal cleavage during the reduction and acid work up of **4** was substantially lower (31% isolated yield of **7** compared to 35% yield of **4**). The difference between yields of polyamino cages and yields of polyimino cages, which increases in the order **4**/**7** < **1**/**6** < **5**/**8** may be explained as follows: (1) A higher number of HN−BH_2 groups per cage requires a longer hydrolysis time to produce a 50% yield of fully hydrolyzed cage under the assumption that the rate of N−BH_2 hydrolysis is identical for all cages. (2) The higher the number of acetal groups per cage, the larger will be the reduction in yield of the final polyamino cage, if *x*% of all acetal groups are cleaved during the hydrolysis step. (3) Acetal cleavage might be in part catalyzed by the ammonium groups of the $CH_2NH_2^+CH_2CH_2NH_2^+CH_2$ linkers (Scheme 2).

The efficiency of this type of catalysis will depend on the conformation of the linkers and the orientation of the ammonium groups, which may differ among the nanocages. Support for intamolecular catalysis comes from the following observation. When a sample of **6**·24CF_3COOH is heated to 80 °C at high vacuum for 24 h, the ^{1}H NMR spectrum of this sample in CD_3-OD shows partial loss of acetal groups.

Solvent Effects. The effect of the bulk solvent on the yield of nanocages **1**, **4**, and **5** is summarized in Table 1. Five different solvents were used in this study. Tetramer **4** is the major

Table 1: Yield[a] (in %) of **1**, **4**, and **5** in the TFA-Catalyzed Condensation of **2** with 2 equiv of **3** in Different Solvents

entry	solvent	1	4	5
1	THF	5[b]	35[b](31)[c]	5[b]
2	$CHCl_3$	82	4−5	0
3	CH_2Cl_2	<5	0	65
4	CH_2ClCH_2Cl	0	0	26
5	$CHCl_2CHCl_2$	17	0	33

[a] Determined by integration of selected product signals in the ^{1}H NMR spectrum of the crude products unless otherwise noted. [b] Determined by HPLC of the $NaBH_4$-reduced reaction mixture. [c] Isolated yield of **7**·16CF_3COOH.

condensation product in THF, hexamer **1** in chloroform, and octamer **5** in dichloromethane, 1,2-dichloroethane, and 1,1,2,2-tetrachloroethane.

It should be noted that GPC of each reaction mixture showed predominant formation of aggregates with a molecular weight equal or very close to that of the major product. For example, even though **5** is only formed in 26% yield in 1,2-dichloroethane, >80% of species have a molecular weight of 7000 ± 1000. With the exception of 1,1,2,2-tetrachloroethane, all other solvents have the ability to strongly stabilize one of the nanocages and to bias the equilibrium toward this cage. Most notable are chloroform and dichloromethane, which strongly favor formation of **1** and **5**, respectively. In these solvents, the free-energy difference between **1** and **5** changes by $\Delta\Delta G >$ 4.1 kcal/mol.

NMR spectroscopic and computational studies by Rebek and co-workers have firmly established that self-assembly of molecular capsules in high yield requires correct space occupancy of the capsule's inner cavity by one or more guest molecules, which could be solvent, an additive, or both.[26] Rebek's 55% occupancy rule applies not only to capsules formed via hydrogen bonding, but also to metal coordination cages and to covalently linked hemicarcerands and carcerands. The presence of large portals in each of the nanocage shells, through which part of the cavity occupying solvent can easily protrude to optimize the packing in the inner cavity, makes it unlikely that space occupancy is solely responsible for the solvent effects reported in Table 1. We believe that the major contribution to these solvent effects arises from improper solvation of the flexible linkers in minor nanocage products as a consequence of the confined space inside the cavities and inside the openings in the host shells. The different geometric features of the three nanocages will influence the ability of solvent that is located in the inner cavity or inside an opening in the host shell to properly interact with the linker groups. In fact, a solvation energy difference of less than 0.1 kcal/mol per imine bond is needed to explain the different yields in each solvent.

Mechanistic and Energetic Aspects of Nanocage Formation. Careful analysis of NMR spectra of the condensation in $CHCl_3$ taken periodically revealed a larger amount of **4** (approximately 17 and 10% of **1**) at the initial stage of the reaction (30 min). Subsequently, the concentration of **4** decreased whereby the amount of hexamer **1** increased until an equilibrium composed of about 82% of **1** and approximately 5% of **4** is reached. A similar observation was made in CH_2Cl_2. After short reaction time (3 h), the reaction mixture contained approximately 15% hexamer **1** and 5% octamer **5**. Over the next 1.5 days, the ratio **1**:**5** slowly inverted to reach the final equilibrium composition of 65% **5** and 5% **1**. In these solvents, the smaller nanocapsules are kinetic products simply because collection of less components and the correct formation of fewer imine bonds is required to form a smaller as opposed to a larger capsule.

GPC analysis of these reaction mixtures further shows that the system rapidly grows to an assembly of oligomeric compounds composed of 4−9 cavitands (molecular weight range 4000−9000). Upon further reaction, the molecular weight distributions of the products/intermediates slowly narrow until they reach the final distributions shown in Figure 2. Larger oligomeric aggregates with MW > 15000 do not form at any stage of the reaction most likely due to the more unfavorable entropy associated with polymer formation as opposed to the formation of smaller spherical capsules.

Among the condensation products, linear oligomers or 2D sheets were not observed. This is not surprising because these possible products have unreacted formyl and amino groups at their ends or periphery, which will disfavor them by $\Delta G > 4$ kcal per mol of unreacted amine/aldehyde compared to a cage that is composed of the same number of building blocks. This energetic penalty was estimated from the equilibrium constant K_{298K} = [formed imine bonds] × [H_2O]/([unreacted formyl groups] × [unreacted *n*-butylamine]) = 770 ± 50 for the reaction between cavitand **2** and 4 equiv of *n*-butylamine in $CDCl_3$, which corresponds to $\Delta G = -3.9$ kcal/mol ($\Delta H = -6.5$ kcal/mol; $\Delta S = -8.5$ cal/mol/K).[27] For the same reason, dynamic covalent libraries of ditopic building blocks are composed predominately of closed macrocyclic products rather than linear oligomers.[19a,28,29]

The absence of octaiminohemicarcerand **VI** (X = CH_2CH_2), which is the entropically most favorable capsule, and the preferential formation of capsules built-up from 4 to 8 cavitands can be understood based on the structural features of the building blocks (Scheme 3). In octaiminohemicarcerands **VI**, both cavitands are coplanar to each other, which requires kinked or twisted diamines. Ethylene-1,2-diamine would have to adopt a gauche conformation to arrange both cavitands in **II** in this conformation. On the other hand, in the favorable anti conformation, both cavitands are nearly perpendicular to each other (**I**), which is close to the orientation of neighboring cavitands in **III**, **IV**, and **V**. In fact, diamines that have a low energy kinked conformation or which do not require twisting, such as $H_2N(CH_2)_3NH_2$,[1] $H_2N(CH_2)_5NH_2$, 1,3-$(H_2N)_2C_6H_4$,[17] 1,4-$(H_2NCH_2)_2C_6H_4$ and 1,3-$(H_2NCH_2)_2C_6H_4$, or in which the required torsional twist of the alkyl chain is distributed over several bonds, such as $H_2N(CH_2)_4NH_2$,[1] yield hemicarcerands **9**−**14** in essentially quantitative yield upon reacting with **2** (Scheme 4).

(26) Mecozzi, S.; Rebek, J., Jr. *Chem.−Eur. J.* **1998**, *4*, 1016−1022.
(27) K_{298K} was determined from the ^{1}H NMR spectrum of **2** (7.1 mg) and 4 equivalents of *n*-butylamine in $CDCl_3$ containing 0.04 equivalents TFA and was calculated from the relative integration of the unreacted formyl protons (δ 10.4−10.2), all imine protons (δ 8.0−8.6), water, and the α-methylene protons of unreacted *n*-butylamine. ΔH and ΔS were determined from the temperature dependence of K between 298 and 318 K.
(28) (a) Kamplain, J. W.; Bielawski, C. W. *Chem. Commun*. **2006**, 1727−1729. (b) González-Álvarez, A.; Alfonso, I.; López-Ortiz, F.; Aguirre, Á.; García-Granda, S.; Gotor, V. *Eur. J. Org. Chem*. **2004**, 1117−1127.
(29) (a) Cousins, G. R. L.; Furlan, R. L. E.; Ng, Y.-F.; Redman, J. E.; Sanders, J. K. M. *Angew. Chem. Int. Ed*. **2001**, *40*, 423−428. (b) Brisig, B.; Sanders, J. K. M.; Otto, S. *Angew. Chem., Int. Ed*. **2003**, *42*, 1270−1273. (c) González-Álvarez, A.; Alfonso, I.; Gotor, V. *Chem. Commun*. **2006**, 2224−2226.

Scheme 3. Design Principles for the Thermodynamically Controlled Multicomponent Synthesis of Nanocages (III−V) and Octaiminohemicarcerands (VI)

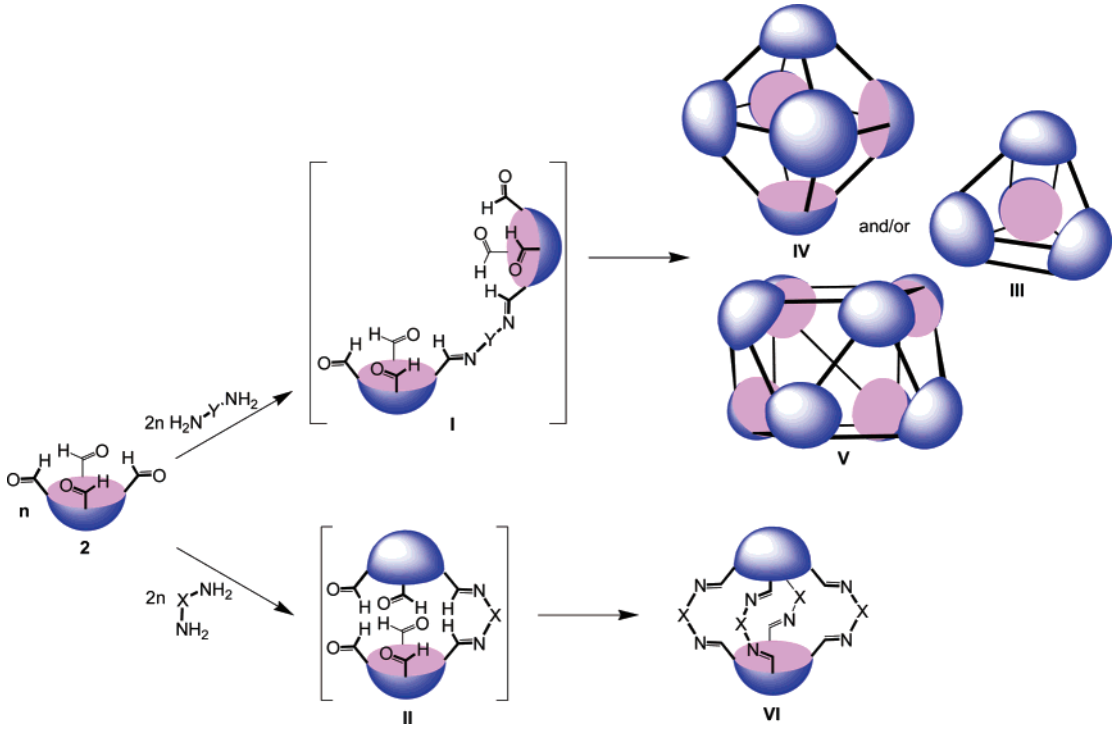

Scheme 4. Examples of Octaiminohemicarcerands Formed via the Condensation of **2** with 2 equiv of a Diamine $H_2N-X-NH_2$

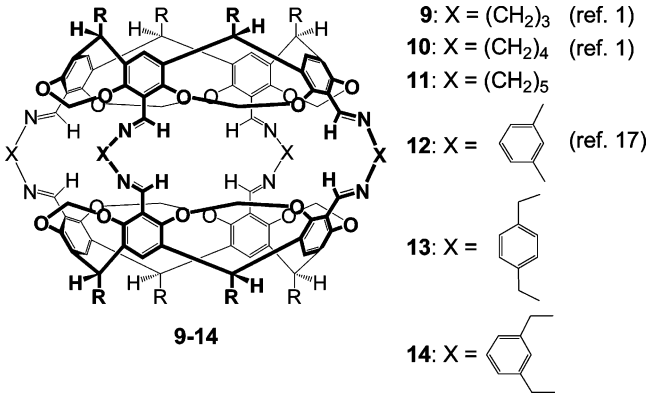

Thus, the outcome of multicomponent condensation reactions between cavitand **2** and diamines depends on the balance between entropy costs associated with collecting 3*n* reactants, the amount of strain in the linker groups, and the energetics of host solvent interactions. The latter can be used to fine-tune a particular system, similarly to the amplification effect of templates on dynamic combinatorial receptor libraries.[19,29,30]

Conclusions

We have shown that nanoscaled container molecules can be prepared in one pot through thermodynamically controlled multicomponent reactions between cavitand **2** and ethylene-1,2-diamine **3**. The outcome of these reactions can be fine-tuned by the solvent and gives predominately tetrahedral **4** in THF, octahedral **1** in $CHCl_3$, and square antiprismatic **5** in CH_2Cl_2. The formation of larger containers composed of four, six, or eight cavitands can be rationalized with the geometry of cavitand **2**, the relative orientation of two cavitands in these containers and the preferred anti conformation of **3**. Thus, linear diamines are expected to yield larger nanocontainers in high yield, whereas kinked diamines give octaiminohemicarcerands. The latter is consistent with the quantitative one-pot synthesis of hemicarcerands **9**−**14**. On the basis of the design principle outlined in Scheme 3, many other hemicarcerands and nanocages should be accessible in high yield via one-pot multicomponent reactions between **2** or related cavitands and appropriate diamines.

Finally, we note an interesting close similarity between the dynamic reactions of **2** and **3** and the self-assembly behavior of pyrogallo[4]arenes. The latter self-assemble into spheroidal hexameric hydrogen bonded capsules similar to **1**, which have been structurally characterized in solution and in the solid state.[31] However, in the presence of various polyaromatic additives, pyrogallo[4]arene orders itself into a nanotubular array in the solid state.[32] These nanotubes are composed of octameric pyrogallo[4]arene segments that are structurally similar to **5** and **8**. Covalent linkage of multiple cages **8** face-to-face could yield covalent analogues of these nanotubes described for pyrogallo-[4]arene.

Experimental Section

General. All reactions were conducted under argon. Reagents and chromatography solvents were purchased from Aldrich and used without further purification. NMR spectra were recorded on Varian 300 or 400 MHz FT-NMR spectrometers. ^{1}H NMR spectra recorded in $CDCl_3$ or CD_3OD were referenced to residual $CHCl_3$ and CHD_2OD at 7.26 and 3.30 ppm, respectively. ^{13}C NMR spectra recorded in $CDCl_3$ or CD_3OD were referenced to $CDCl_3$ and CD_3OD at 77.0 and 49.0 ppm,

(30) Severin, K. *Chem.−Eur. J.* **2004**, *10*, 2565−2580.
(31) (a) Gerkensmeier, T.; Iwanek, W.; Agena, C.; Fröhlich, R.; Kotila, S.; Näther, C.; Mattay, J. *Eur. J. Org. Chem.* **1999**, *9*, 2257−2262. (b) Atwood, J. L.; Barbour, L. J.; Jerga, A. *Proc. Natl. Acad. Sci. U.S.A.* **2002**, *99*, 4837−4841.
(32) Dalgarno, S. J.; Cave, G. W. V.; Atwood, J. L. *Angew. Chem., Int. Ed.* **2006**, *45*, 570−574.

respectively. Mass spectra were recorded on an Applied Biosystems Voyager DE-Pro mass spectrometer in reflectron mode (MALDI-TOF). 2,4,6-Trihydroxylacetophenone (THAP) was used as matrix. Positive molecular ions are usually detected as proton or sodium adducts for the compounds reported here. Cavitand **2** was prepared as reported earlier.[17]

Octaiminohemicarcerand 11. (Procedure A). Cavitand **2** (33.2 mg, 0.0358 mmol) was added to a solution of 1,5-diaminopentane **16** (7.9 mg, 0.0773 mmol) and trifluoroacetic acid (0.27 μL) in $CHCl_3$ (3 mL). The solution was stirred for 21.5 h at room temperature. The solvent was removed and the yellowish solid product was dried overnight at high vacuum (>95% yield). ^{1}H NMR (300 MHz, $CDCl_3$, 25 °C): δ = 8.35 (s, 8H; C*H*═N), 7.12 (s, 8 H; aryl-*H*), 5.59 (d, ^2J(H, H) = 7.5 Hz, 8 H; OCH_{outer}HO), 4.86 (t, ^3J(H, H) = 7.8 Hz, 8 H; C$H_{methine}$), 4.42 (d, ^2J(H, H) = 7.2 Hz, 8 H; OCH_{inner}HO), 3.50 (m, 16 H; NCH_2), 2.23−2.17 (m, 16 H), 1.6−1.4 (m, 24 H; NCH$_2$CH_2 CH_2), 1.4−1.2 (m, 48 H), 0.91 (t, 24 H). ^{13}C NMR (75 MHz, $CDCl_3$, 25 °C): δ = 157.2, 153.6, 139.6, 138.7, 129.4, 126.1, 125.4, 124.0, 121.7, 100.8, 66.2, 36.8, 32.3, 30.2, 27.9, 23.1, 14.5. MS (MALDI-TOF) *m*/*z*: 2123.32 (M + H$^+$, 100%); Calcd for $C_{132}H_{169}N_8O_{16}$ + H$^+$: 2123.27.

Octaiminohemicarcerand 13. Application of procedure A with para-xylylene diamine **17** instead of **16** (24.5 h reaction time) gave octaimine **13** as a yellow powder (>95% yield). ^{1}H NMR (300 MHz, $CDCl_3$, 25 °C): δ = 8.33 (s, 8H; C*H*═N), 7.18 (s, 16 H; −C$_6H_4$−), 7.10 (s, 8 H; aryl-*H*), 5.32 (d, ^2J(H, H) = 7.2 Hz, 8 H; OCH_{outer}HO), 4.82 (t, ^3J(H, H) = 7.8 Hz, 8 H; C$H_{methine}$), 4.60 (br s, 16 H; NCH_2), 4.16 (d, ^2J(H, H) = 7.5 Hz, 8 H; OCH_{inner}HO), 2.20 (br s, 16 H), 1.5−1.2 (m, 48 H), 0.91 (t, ^3J(H, H) = 6.9 Hz, 24 H). ^{13}C NMR (75 MHz, $CDCl_3$, 25 °C): δ =157.2, 153.4, 138.6, 138.3, 128.2, 124.0, 121.6, 99.8, 66.2, 36.6, 32.2, 30.1, 27.8, 23.0, 14.5. MS (MALDI-TOF) *m*/*z*: 2258.90 (M + H$^+$, 100%); Calcd for $C_{144}H_{160}N_8O_{16}$ + H$^+$: 2259.21.

Octaiminohemicarcerand 14. Application of procedure A with meta-xylylene diamine **18** instead of **16** (24.5 h reaction time) gave octaimine **14** as a yellow powder (>95% yield). ^{1}H NMR (300 MHz, $CDCl_3$, 25 °C): δ = 8.44 (s, 8H; C*H*═N), 7.17 (s, 8 H; aryl-*H*), 7.11 (s, 4 H; −C$_6H_4$−), 6.96 (d, ^3J(H, H) = 7.8 Hz, 8 H; −C$_6H_4$−), 6.80 (t, ^3J(H, H) = 7.2 Hz, 4 H; −C$_6H_4$−), 5.48 (d, ^2J(H, H) = 7.2 Hz, 8 H; OCH_{outer}HO), 4.88 (t, ^3J(H, H) = 8.1 Hz, 8 H; C$H_{methine}$), 4.72 (s, 16 H; NCH_2), 4.48 (d, ^2J(H, H) = 7.5 Hz, 8 H; OCH_{inner}HO), 2.25 (m, 16 H), 1.5−1.2 (m, 48 H), 0.93 (t, ^3J(H, H) = 6.9 Hz, 24 H). ^{13}C NMR (75 MHz, $CDCl_3$, 25 °C): δ = 157.2, 153.6, 139.6, 138.7, 129.4, 126.1, 125.4, 124.0, 121.7, 100.8, 66.2, 36.8, 32.3, 30.2, 27.9, 23.1, 14.5. MS (MALDI-TOF) *m*/*z*: 2259.27 (M + H$^+$, 100%); Calcd for $C_{144}H_{160}N_8O_{16}$ + H$^+$: 2259.21.

Tetrameric Capsule 7. A solution of cavitand **2** (255.9 mg, 275 μmol), ethylenediamine **3** (34.0 mg, 566 μmol), and CF_3CO_2H (TFA) (2.17 μL, 29 μmol) in THF (30.0 mL) was stirred at room temperature for 70 h. Then $NaBH_4$ (2.0 g, 52.9 mmol) and MeOH (3.0 mL) were added into the solution while being stirred vigorously. After stirring at room-temperature overnight, the solvent was removed at reduced pressure. The solid was stirred with water (50.0 mL) for 20 min to destroy excess $NaBH_4$ followed by filtration. The precipitate was dissolved in CH_3OH/concentrated HCl (10:1) (165.0 mL). After 4 days at room temperature, the solvent was removed and the crude product was purified by reversed-phase HPLC (Vydac RP-18; 10 μ; 300 Å; 21 × 250 mm; CH_3OH/H_2O/TFA (gradient 85/15/0.1 to 90/10/0.1; 31 min); 10 mL/min; 280 nm; $t_{retention}$(**7**) = 23.9 min), which gave **7**−[CF_3-COOH]$_{16}$ as a white solid (122.4 mg; 31% yield based on **2**). ^{1}H NMR (CD_3OD; 0.4% CF_3COOD; 12.7 °C; 400 MHz): δ_H, 7.55 (br s, 16H, H_{aryl}); 6.45 (d, *J* = 7.2 Hz, 4H, OCH_{out}HO); 6.14 (d, *J* = 7.2 Hz, 8H, OCH_{out}HO); 6.08 (d, *J* = 7.2 Hz, 4H, OCH_{out}HO); 4.86 (m, 16H, CH(CH$_2$)$_4$CH$_3$); 4.58 (d, *J* = 7.2 Hz, 4H, OCH_{in}HO); 4.40 (d, *J* = 7.2 Hz, 8H, OCH_{in}HO); 4.39 (d, *J* = 7.2 Hz, 4H, OCH_{in}HO); 4.26 (d, *J* = 13.3 Hz, 8H, NCH_2Ar); 4.21 (d, *J* = 13.3 Hz, 8H, NCH_2Ar); 4.13 (d, *J* = 12.7 Hz, 8H, NCH_2Ar); 4.02 (d, *J* = 12.7 Hz 8H, NCH_2Ar); 3.60 (m, 32H, N(CH_2)$_2$N); 2.39 (br s, 32H, CHCH_2(CH$_2$)$_3$CH$_3$); 1.6−1.3 (m, 96H, CHCH$_2$(CH_2)$_3$CH$_3$); 0.93 (m, 48H; CHCH$_2$(CH$_2$)$_3$CH_3). ^{13}C NMR (CD_3OD; 25 °C; 100.58 MHz): δ_C, 161.8 (q, ^2J(C, F) = 35.4 Hz, CF_3COO^-), 155.52 (C4), 155.23 (C4), 155.11 (C4), 154.91 (C4), 139.87 (C5), 139.82 (C5), 139.68 (C5), 124.73 (C6), 124.67 (C6), 119.69 (C3), 119.63 (C3), 116.43 (q, ^1J(C, F) = 297 Hz, CF_3COO^-), 101.39 (C7), 101.04 (C7), 100.96 (C7), 44.75 (C1), 44.01 (C1), 42.98 (C2), 42.50 (C2), 38.33 (C8), 38.12 (C8), 32.82 (C10), 32.79 (C10), 30.77 (C9), 30.72 (C9), 30.60 (C9), 28.86 (C11), 28.83 (C11), 23.85 (C12), 14.40 (C13). MS (MALDI-TOF) *m*/*z*: 3941.85 (M + H$^+$, 100%); Calcd for $C_{240}H_{320}N_{16}O_{32}$ + H$^+$: 3941.40. Elemental analysis: calcd. for $C_{272}H_{346}F_{48}N_{16}O_{69}$ (**7**·16CF_3CO_2H-5H_2O): C, 55.79; H, 5.96; N, 3.83; found: C, 55.77; H, 5.87; N, 3.58.

Octameric capsule 8. A solution of cavitand **2** (362.1 mg, 389.5 μmol), ethylenediamine **3** (47.4 mg, 788.7 μmol), and CF_3CO_2H (TFA) (3.0 μL, 40.5 μmol) in CH_2Cl_2 (30.0 mL) was stirred at room temperature for 44 h. $NaBH_4$ (6.0 g, 158.6 mmol) and MeOH (4.0 mL) were added to the solution with vigorous stirring. The suspension was stirred at room temperature overnight. The solvent was removed at reduced pressure. The residue was suspended in water (100.0 mL) and stirred for 20 min to destroy excess $NaBH_4$ followed by filtration. The residue was dissolved in CH_3OH/concentrated HCl (10:1) (135.0 mL). After 4.5 days at room temperature, the solvent was removed and the crude product was purified by reversed-phase HPLC (Vydac RP-18; 10 μ; 300 Å; 21 × 250 mm; CH_3OH/H_2O/TFA (gradient 85/15/0.1 to 98/2/0.1; 80 min); 10 mL/min; 280 nm; $t_{retention}$(**8**) = 58.7 min), which gave **8**·[CF_3COOH]$_{32}$ as a white solid (137.6 mg; 25% yield based on **2**). ^{1}H NMR (CD_3OD; 0.4% CF_3COOD; 25 °C; 400 MHz) δ_H, 7.55 and 7.54 (32H, H_{aryl}); 6.17 (m, 32H, OCH_{out}HO); 4.86 (m, 32H, CH(CH$_2$)$_4$CH$_3$); 4.46 (m, 32H, OCH_{in}HO); 4.16 (m, 64H, NCH_2Ar); 3.61 (s, 32H, N(CH_2)$_2$N); 3.57 (s, 32H, N(CH_2)$_2$N); 2.38 (br s, 64H, CHCH_2(CH$_2$)$_3$CH$_3$); 1.6−1.2 (m, 192H, CHCH$_2$(CH_2)$_3$CH$_3$); 0.93 (t, *J* = 7.1 Hz, 96H, CHCH$_2$(CH$_2$)$_3$CH_3). ^{13}C NMR (CD_3OD; 25 °C; 100.58 MHz) δ_C, 162.14 (q, ^2J(C, F) = 36 Hz, CF_3COO^-), 155.29 (C4), 155.21 (C4), 155.19 (C4), 155.15 (C4), 139.92 (C5), 139.86 (C5), 139.84 (C5), 124.66 (C6), 119.73 (C3), 119.65 (C3), 117.75 (q, ^1J(C, F) = 295 Hz, CF_3COO^-), 101.14 (C7), 100.97 (C7), 44.51 (C1), 44.26 (C1), 42.55 (C2), 42.51 (C2), 38.35 (C8), 32.93 (C10), 32.89 (C10), 32.86 (C10), 30.74 (C9), 28.91 (C11), 28.85 (C11), 23.83 (C12), 14.41 (C13). MS (MALDI-TOF) *m*/*z*: 7883.38 (M + H$^+$, 100%); Calcd for $C_{480}H_{640}N_{32}O_{64}$ + H$^+$: 7882.81. Elemental analysis: calcd for $C_{544}H_{770}F_{96}N_{32}O_{177}$ (**8**·32CF_3CO_2H-49H_2O): C, 52.63; H, 6.25; N, 3.61; found: C, 52.65; H, 6.07; N, 3.60.

Gel Permeation Chromatography. Gel permeation chromatography was performed on a Varian Rainin Dual Pump HPLC system equipped with dual wavelength UV/Vis detector, Eppendorf CH-30 column heater, and a Jordi GPC column (cross linked DVB; 10^3 Å pore size; MW cutoff ~25 000; 7.8 mm × 30 cm) with CH_2Cl_2/1% NEt_3 as mobile phase at 60 °C and a flow of 1 mL/min. Approximate molecular weights of analytes were determined from a semilogarithmic calibration plot (ln(MW) against retention time) using benzene (MW 78); cavitand **2** (MW 928); a NMP hemicarceplex (MW 2348)[33] and **6** (MW 5912) as molecular weight standards.

Acknowledgment. We warmly thank the National Science Foundation for support of this research (Grant CHE-0518351).

Supporting Information Available: ^{1}H and ^{13}C NMR spectra of compounds **7**·16CF_3CO_2H and **8**·32CF_3CO_2H, **11**, **13**, and **14** and of crude reaction mixtures. TOCSY of **5** and **8**. Mass spectra of compounds **6**, **7**, **8**, and of crude reaction mixtures. Gel permeation chromatograms of crude condensation mixtures. This material is available free of charge via the Internet at http://pubs.acs.org.

JA0644733

(33) Warmuth, R.; Maverick, E. F.; Knobler, C. B.; Cram, D. J. *J. Org. Chem.* **2003**, *68*, 2077−2088.